Thermal modification of microstructures and grain boundaries in silicon carbide

Xiao Feng Zhang[1], and Lutgard C. De Jonghe[1,2]

[1] Materials Sciences Division, Lawrence Berkeley National Laboratory
University of California, Berkeley, CA 94720

[2] Department of Materials Science and Mineral Engineering
University of California, Berkeley, CA 94720

Abstract

Polycrystalline SiC samples hot-pressed with aluminum, boron, and carbon sintering additions (ABC-SiC) were characterized using transmission electron microscopy. The study focused on the effects of high temperature treatment on microstructure. Three temperatures were found critical at which considerable microstructural changes took place. At a threshold temperature of ~1000°C, 1 nm-wide, amorphous intergranular films started to crystallize. At ~1300°C, lattice diffusion in SiC grains resulted in nanoprecipits which could diffuse into grain boundaries and significantly altered composition there. Quantitative microanalysis revealed doubled Al content in intergranular films after annealing at 1300°C. Except crystallization in intergranular films and nano-precipitation in matrix grains, microstructure remained stable until 1600°C, at which microstructural changes with volatile features. A brief holding at 1900°C brought marked changes in microstructure, including structural change in intergranular films, dissolved nanoprecipitates, unit cell dilation, and cracking. The results indicate that ABC-SiC is highly promising in structural applications at up to 1500°C.

Keywords: Ceramic, Annealing, Microstructure, Grain boundaries, TEM.

I. INTRODUCTION

SiC possesses many attractive properties such as low density and thermal expansion coefficient, good in thermal conductivity, hardness, elastic modules, flexural strength, and thermal shock resistance. However, the use of SiC to date has been limited by its low fracture toughness (K_{Ic}, ~2-5 MPa.m$^{1/2}$ for commercially available materials). Various attempts have been made to improve toughness, including reinforcement with alumina-coated SiC platelets,[1] and *in situ* toughening. The *in situ* toughening mechanism, which was effective for Si_3N_4 ceramics,[2,3] also led to significantly enhanced toughness for SiC.[4] A microstructure containing elongated, plate-like SiC grains was produced by hot pressing mixture of α-SiC with Al_2O_3 and Y_2O_3,[5] while β-SiC hot-pressed with aluminum, boron, and carbon additives (ABC-SiC) led to further enhancement of the fracture toughness.[4] In the latter, liquid phases were formed at processing temperatures, leading to the formation of residual intergranular films (IGFs).[4,6-11] The nature of these amorphous intergranular films was shown to consist mainly of Al-O-Si-C[11] or Al-O-C,[12,13] and to provide a path for intergranular crack propagation. Elastic bridging and pullout of the interlocked SiC grains[4,5,14] contributed to the toughening,[2,15-17] leading to fracture toughness of as high as 9 MPa.m$^{1/2}$ for ABC-SiC.[4]

In general, it can be expected that glassy grain-boundary films in ceramic materials benefit room temperature toughness but degrade high temperature properties due to their softening. However, extensive mechanical studies demonstrated positive responses of ABC-SiC to high temperature exposure.[18-25] This enhancement in mechanical performance is likely a consequence of structural and chemical modifications that result from the heat treatments. In this paper, we report on the effects of the thermal treatment on microstructure of ABC-SiC.

II. EXPERIMENTAL

Materials Processing

Submicron β-SiC (B20, H. C. Starck, Germany) powder was mixed with 3 wt% aluminum (H-3 and H-10, Valimet, Stockton, CA), 0.6 wt% boron (Callery Chemical Co, Callery, PA), and 2 wt% carbon sintering additives. Apiezon wax (AVO Biddle Instruments, Blue Bell, PA) was dissolved in toluene to serve as the carbon source, and then

Al, B, and β-SiC powders were added. The slurry was ultrasonically agitated, stir dried, sieved through a 200 mesh screen, and uniaxially pressed at 35 MPa. Hot-pressing was conducted in an argon atmosphere at 1900°C, at 50 MPa, for 1 hour. 38 mm diameter and 4 mm thick disks were produced, containing polycrystalline SiC dominated by α–4H and α–6H phases. The samples were referred to as ABC-SiC. High density (>99%), high bend strength (typically a 660 MPa MOR) and a reproducible fracture toughness of 5 to 7 $MPa.m^{1/2}$ were achieved without further post-treatment.

Thermal Treatment

The as-hot-pressed ABC-SiC samples were heat-treated in a tungsten mesh furnace under flowing Ar, at temperatures ranging between 800 to 1600°C, for 5 to 840 hrs. Heating rates to 800°C were 10°C/min, and 4°C/min to any higher temperatures. One of the samples was first annealed at 1500°C for 168 hrs and cooled to room temperature, followed by a brief reheating to 1900°C with a 5 min dwell. All samples were examined using transmission electron microscopy (TEM).

TEM Characterization

3 mm disks were cut from the SiC bulks, perpendicular to the hot pressing direction, mechanically ground and polished, dimpled, and thinned to electron transparency by Ar ion beam milling. The areas to be investigated by TEM were further than 100 □m from the surface of the hot-pressed samples. One exception was for the SiC sample annealed at 1900°C. In this case, the near-surface features were of particular interest, since evaporation of some material could lead to additional structural and chemical changes.[26] Therefore, after the 1900°C treatment, TEM samples were prepared by thinning only from one side to allow examination of the near-surface region.

The structural and chemical characterizations were carried out in a Philips CM200 field-emission gun transmission electron microscope operating at 200 kV. For compositional determinations, a 3.5 to 10 nm probe, a windowless detector with an X-ray energy-dispersive spectroscopy (EDS) system, and ES Vision 4.0 software issued by EMISPEC System, Inc. were used. The methodology for quantifying compositions of the nanometer-wide SiC grain boundary films have been described in detail previously.[11-27]

III. RESULTS

Thermal Treatments at 800 to 1600°C

Fig. 1 shows the general microstructure of the as-hot-pressed ABC-SiC. α-SiC grains, with a width of 1 to 3 μm, and an aspect ratio between 2 and 5, constitute about 90 % of the elongated SiC grains. Equiaxed β-SiC grains were also present, with a size generally below 1 μm. Amorphous IGFs were prevalent with a typical width of about 1 nm.[11] EDS microanalyses by Zhang *et al*. determined that the majority of the amorphous IGFs contained Al-O-Si-C constituents.[11,27] The oxygen in IGFs came most likely from oxide surface layers on the SiC starting powder. As a rough estimate, formation of 1 nm-wide Al-O-Si-C grain boundary films in the sintered SiC could result from a 0.1 nm thick SiO_2 surface layer on the starting powder. While the SiO_2 thickness on as-received SiC powder is typically on the order of 5 nm,[28] there is sufficient oxygen to form not only the IGFs but also various oxygen-rich secondary phases.[29]

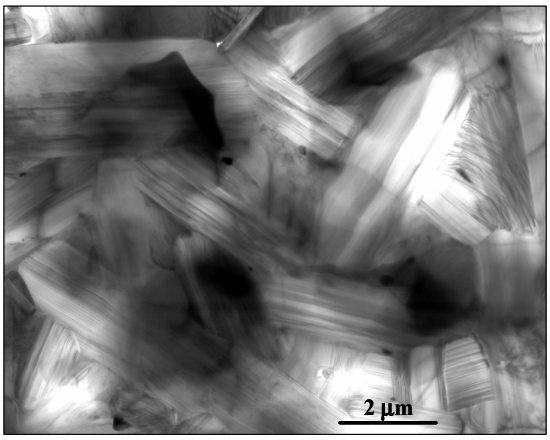

Fig. 1: General microstructural morphology of as-hot-pressed ABC-SiC.

Annealing at 800 to 1000°C did not lead to discernable microstructural changes. However, when subjected to post-annealing at or above 1000°C, the amorphous IGFs started to crystallize. Fig. 2 shows high-resolution images for three different IGFs in a sample annealed at 1000°C for 5 hrs. An amorphous IGF is seen in Fig. 2a and a fully ordered IGF in Fig. 2c. Fig. 2b shows a partially ordered IGF structure. The range of IGF structures in Fig. 2 indicated that the crystallization of the amorphous IGFs was initiated at

about 1000°C Holding the samples at 1000°C for 5-30 hrs transformed about half number of the amorphous IGFs into more ordered structures. Annealing at higher temperatures for prolonged times crystallized the IGFs fully, as reported earlier, as an aluminosilicate with a 2H-wurtzite structure.[11]

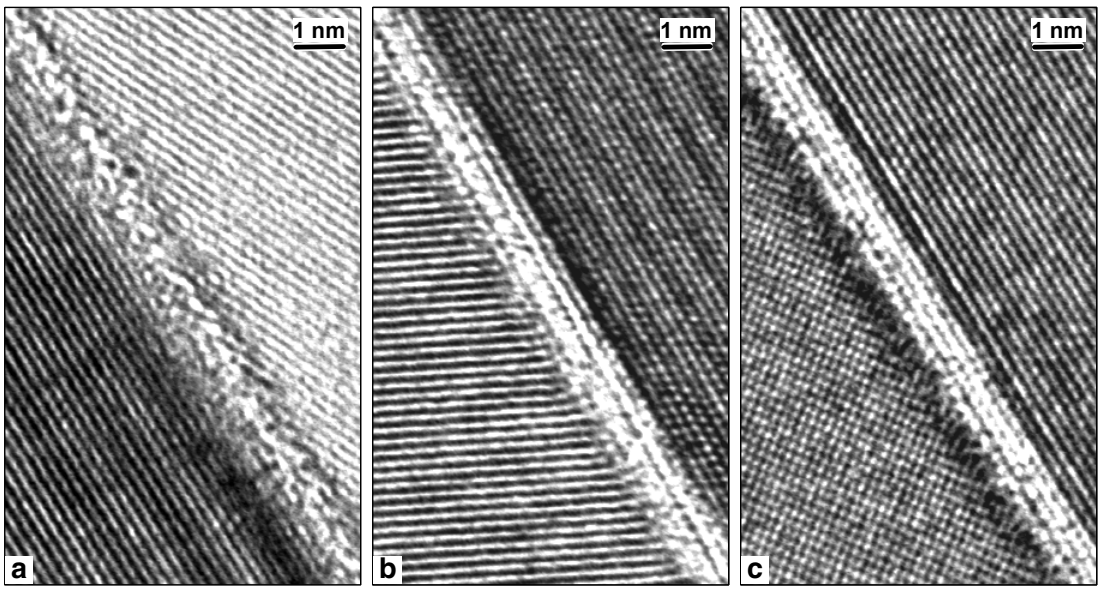

Fig. 2: Three high-resolution images taken from an ABC-SiC sample annealed at 1000°C for 5 hrs. IGFs with (a) amorphous, (b) partially ordered, and (c) crystallized structures can be seen.

To confirm the IGF crystallization process at elevated temperatures, an ABC-SiC sample was heated *in-situ,* in a 300 kV JEOL 3010 transmission electron microscope equipped with a hot stage. Fig. 3 shows high-resolution images for *the same* IGF area before and after *in-situ* heating. The amorphous IGF prior to heating, Fig. 3a, shows localized crystallization after 25 hrs at 1200°C, Fig. 3b. The crystallization tended to proceed epitaxially on the (0001) plane of the adjacent 6H-SiC matrix grain, with a 2H-wurtzite structure similar to that found in furnace-annealed SiC samples. No discernable features could be identified as potential preferential sites for nucleation at the SiC /IGF interface. Presumably, local compositional fluctuations in the IGF serve as nucleation sites.

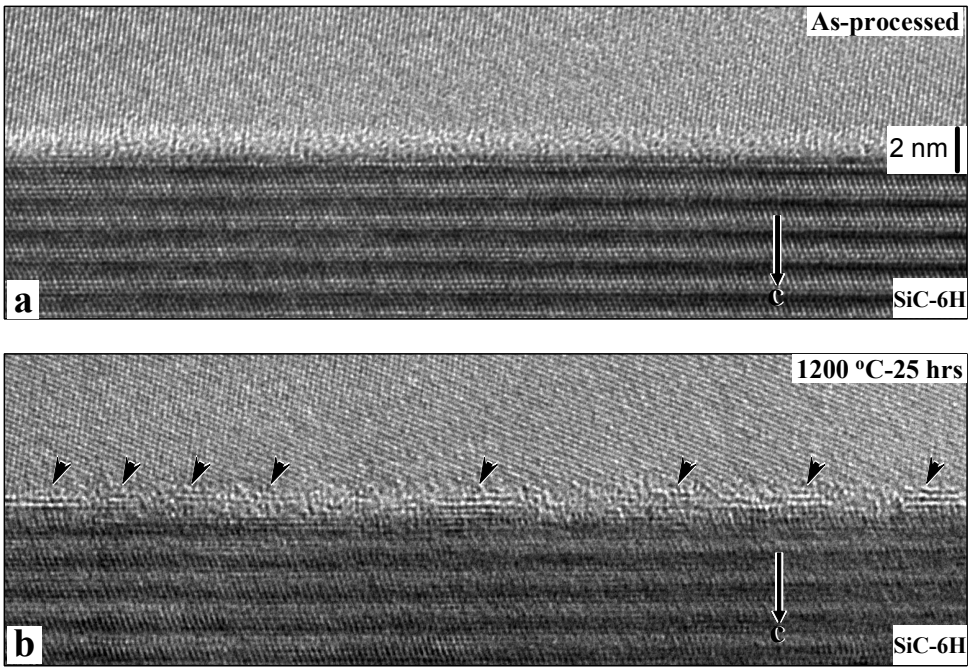

Fig. 3: (a), High-resolution image of an amorphous IGF in as-hot-pressed ABC-SiC. (b), The same IGF area as in (a) but after in-situ heating in a transmission electron microscope at 1200°C for 25 hrs. Arrows indicate the discrete, crystallized IGF segments. The high-resolution image in (b) was taken at room temperature.

Another significant consequence of the thermal treatment was nano-precipitation within SiC matrix grains, as seen in Fig. 4. Although Fig. 4 was taken from a sample annealed at 1400°C, the plate-like nanoprecipitates already formed at 1300°C. The projected dimension of the precipitates after 1300°C annealing is ~4 × 1 nm^2 with a volumetric number density of $5 \times 10^{22}/m^3$. The precipitates coarsened with annealing temperature, accompanied by decrease in the number density. Detailed high-resolution electron microscopy characterization and nano-probe EDS analysis determined an Al_4C_3-based structure and composition with Si and B solutions for the nanoprecipitates. The formation of the precipitates was a consequence of diffusion-controlled classic nucleation and growth.[21,23] Direct evidence for Al lattice diffusion trough the SiC was the formation of precipitate-depletion zones along the grain boundaries, Fig. 4. The precipitate-depletion zones broadened with increasing annealing temperature, allowing an estimate of Al transport rates through SiC grains: ~10^{-17} cm^2/sec at 1400°C.[21,23]

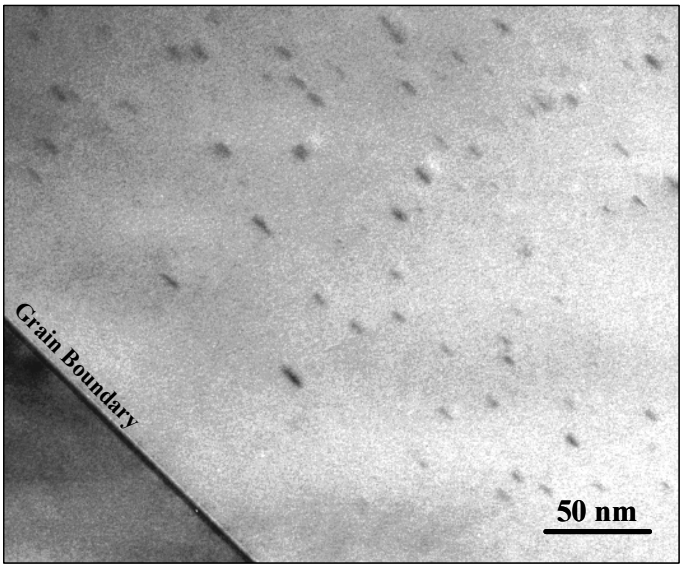

Fig. 4: Nanoprecipitates formed in an ABC-SiC sample annealed at 1400°C. Precipitate-depletion zone along the grain boundary can be seen.

The diffusion of the solutes in SiC lattice changed the grain boundary composition. Since boron is too light to be accurately quantified by EDS, and Si and C signals are inevitably interfered with signals from adjacent SiC grains, the systematic change of the Al content in IGFs as a function of annealing temperature was analyzed with EDS. The results are plotted in Fig. 5, in which one can notice that Al solution in SiC grains decreased at 1100°C and especially at above 1300°C, consistent with TEM observations that Al solutions exsolved from SiC lattice to form nanoprecipitates. Not surprisingly, the Al site density in the grain boundaries (N_{Al}^{GB}) changed as well upon annealing. Despite the large standard deviations, some conclusions can still be drawn. For example, N_{Al}^{GB} for the samples annealed at 1000-1200 °C remained essentially unchanged. It can be derived that the composition of IGFs was invariant between 1000°C and 1200°C, while the IGF crystallized. The N_{Al}^{GB} value was doubled at 1300°C, accompanied by a 20-45% decrease of the grain boundary width. This Al site density is in agreement with $Al_{1.1}Si_{0.9}OC$, a solid solution between 2H-wurtzite Al_2OC and SiC.[30] At even higher annealing temperatures up to 1600°C, both N_{Al}^{GB} and the grain boundary width changed marginally, taking the standard deviation into account. The decrease in grain boundary width can be understood in part as a volume contraction of the IGFs due to amorphous-to-crystalline transformation, and exsolution of SiC onto the adjacent grain surfaces. The significant increase in Al

content in IGFs at 1300°C can be readily correlated with diffusion of the Al-rich chemical species into the grain boundary films (Fig. 4). At higher than 1300°C, the Al content in IGFs became more or less saturated.

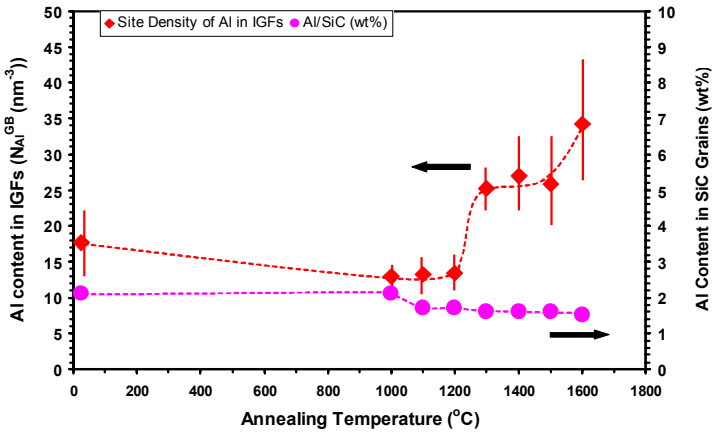

Fig. 5: Plots of EDS-determined Al site density in grain boundary films (N_{Al}^{GB}) and in SiC matrix grains (Al/SiC, wt%) as a function of annealing temperature. Standard deviations are given.

In addition to microstructural and compositional changes in the intergranular films, annealing at 1400°C or above for a prolonged time also resulted in local dissolution of SiC grains and secondary phases, as evidenced by SiC grains with faceted edges as well as triple-junction particles with round corners. Further phase separation also occurred within some secondary phase particles, as shown in Fig. 6. Secondary phase particles became volatile at 1600°C, leaving a large number of empty triple-pockets, Fig. 7.

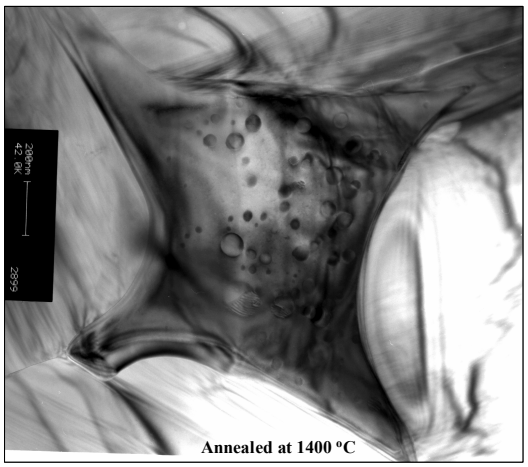

Fig. 6: A secondary-phase particle in the 1400°C-annealed sample. Note the second phase separation within the particle.

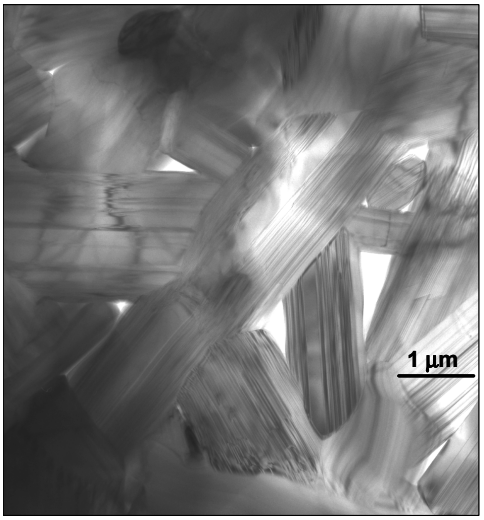

Fig. 7: Empty triple-pockets observed in ABC-SiC samples after the thermal treatment at 1600°C. Note the 100% occupied triple-pockets in as-hot-pressed samples, Fig. 1.

Summarizing the TEM results for the annealing temperatures between 800 and 1600°C, we have found that grain boundary diffusion became significant at about 1000°C, resulting in amorphous-to-crystalline transformation in IGFs. The lattice diffusion in SiC became significant at about 1300°C, as evidenced by the appearance of the nanoprecipitates and precipitate-depletion zones in the vicinity of grain boundaries. Heating at 1600°C had remarkable influences on secondary phase particles.

Thermal treatment at 1900 °C

Crystallization of IGFs can be expected to affect mechanical properties such as high temperature creep.[24] The stability of the crystallized grain boundary films at high temperatures is therefore of interests. As a test, an as-hot-pressed ABC-SiC sample was first annealed in argon, at 1500°C, for 168 hrs, to crystallize the IGFs. After cooling, a slice of this sample was further subjected to heating at 1900°C, for 5 min, in the same environment. Fig. 8 compares high-resolution images of IGFs in the as-hot-pressed, the 1500°C-annealed, and the 1900°C-treated samples. As expected, the amorphous IGF in the as-hot-pressed sample (Fig. 8a) was crystallized at 1500°C (Fig. 8b). After subsequent firing at 1900°C, high-resolution electron microscopy showed an amorphous structure (Fig. 9c) for ~39 % out of 23 IGFs examined, while another 61 % were crystalline IGFs (Fig. 9d). These percentages significantly differed from that in the as-hot-pressed and 1500°C-annealed samples. For example, 86% IGFs examined in the 1500°C-annealed SiC were crystalline, while about the same fraction of IGFs were amorphous in the as-hot-pressed samples. The 39:61 ratio obtained in the 1900°C-treated samples suggested that the treatment at 1900°C re-melted ~25% of the crystallized IGFs. It was also noticed that the mean value for the width of the disordered IGFs was reduced by about 44 % with respect to that of the as-hot-pressed samples.

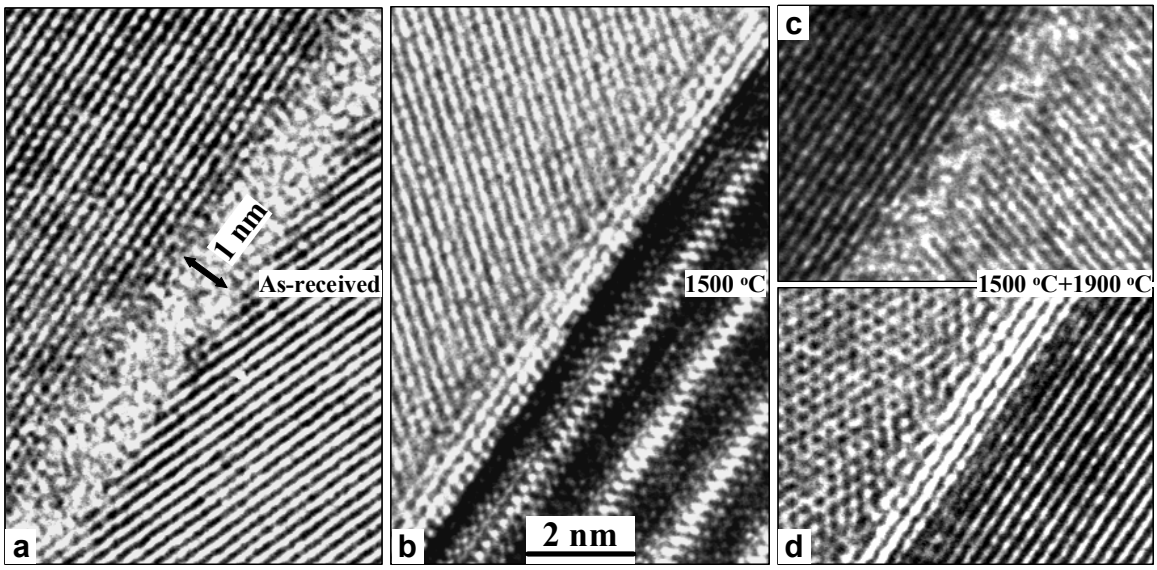

Fig. 8: High-resolution micrographs obtained from (a), the as-hot-pressed sample, (b), the 1500°C-annealed sample, (c) and (d), the 1900°C-treated sample. The 1500°C treatment crystallized the amorphous IGF, while the subsequent brief holding at 1900°C re-melted some crystalline IGFs. Note that the images were not taken from the same IGF.

EDS spectra showed the same elemental constituents in IGFs in the 1500°C- and the 1900°C-treated samples. Particularly, Al and O peaks were readily detectable in both samples. Detailed EDS quantification was performed to determine the Al concentration in SiC grains (Al/SiC wt%), the Al excess in grain boundary films (Γ_{Al}, defined as Al atom excess per grain boundary area with respect to that in SiC), as well as the C/Si atom ratio in SiC grains. The results are summarized in Table I. It can be seen that Γ_{Al} values obtained from the 1500°C- and the 1900°C-treated samples are close, indicating the existence of the Al-rich IGFs even after the 1900°C treatment, therefore confirming the high-resolution observation of the IGFs in Fig. 8. C/Si atom ratios in both samples are close to the unity; therefore, no stoichiometry changes SiC develop as a result of this treatment.

Table I: EDS-determined Al concentration in SiC grains (Al/SiC wt%), Al excess in grain boundary films (Γ_{Al}), as well as C/Si atom ratio in samples annealed at 1500°C and the same bulk piece subsequently fired at 1900°C. Statistical mean values are listed with standard deviations.

Samples ABC-SiC	**Al/SiC** (wt%)	**Γ_{Al}** (nm^{-2})	**C/Si** (atom ratio)
1500°C-168 hrs	1.6±0.2	19.7±9.5	1.23±0.20#
1900°C–5 min.	1.4±0.1	16.4±4.5	0.94±0.36

#Hydrocarbon contamination during EDS spectrum acquisition caused a greater C/Si mean value.

Selected-area electron diffraction was performed on SiC grains to detect possible change in lattice parameters caused by the 1900°C heating. The diffraction analyses were concentrated on α-4H and α-6H major phases in ABC-SiC. The results are given in Table II. It can be seen that in comparison with the as-hot-pressed ABC-SiC, annealing at 1500°C resulted in virtually no changes in lattice parameters within the experimental errors. However, exposure to 1900°C for 5 min. substantially dilated the hexagonal unit cells. The unit cells of 4H and 6H phases expanded by 12.4±9.9 %, and 5.2±4.5 %, respectively. Curiously, the unit cells in 4H and 6H phases dilated along the different directions. The 4H phase expanded mainly in the hexagonal basal planes, whereas the 6H phase expanded

mostly along the *c*-direction. The fact that the unit cell dilation was observed at room temperature indicates that the expansion of the unit cell at 1900°C in argon was irreversible on cooling.

Table II: Lattice parameters determined using selected-area electron diffraction. 4H- and 6H-SiC grains were analyzed. Experimental errors are adopted. Volume dilation for the unit cells after annealing is calculated with respect to the as-hot-pressed samples.

ABC-SiC	**α-4H ($P6_3mc$)**	**α-6H ($P6_3mc$)**
As-Hot-Pressed		
a (Å)	3.07±0.03	3.06±0.03
c (Å)	10.03±0.21	14.89±0.38
1500°C-168 hrs		
a (Å)	3.08±0.03	3.08±0.03
c (Å)	9.99±0.21	15.02±0.24
Volume Dilation	Negligible	Negligible
1900°C-5 min#		
a (Å)	3.19±0.04	3.06±0.03
c (Å)	10.44±0.23	15.66±0.26
Volume Dilation	12.4±9.9 %	5.2±4.5 %

#From the same bulk sample first annealed at 1500°C for 168 hrs and cooled.

In addition to change of the IGF structure and unit cell dilation in the ABC-SiC after the 1900°C thermal treatment, dissolution of the nanoprecipitates that formed at lower temperatures, and evaporation of second-phase particles were also observed. The dissolved nanoprecipitates did not diffuse into SiC lattice. Some of these changes such as unit cell dilation could cause stress and cracking. The micrograph in Fig. 9 shows cracks in the sample after the 1900°C thermal treatment. It should be emphasized that some microstructural changes observed in the 1900°C-treated sample could be surface-related because the corresponding TEM sample was sectioned from a within 100 μm depth from the bulk surface.

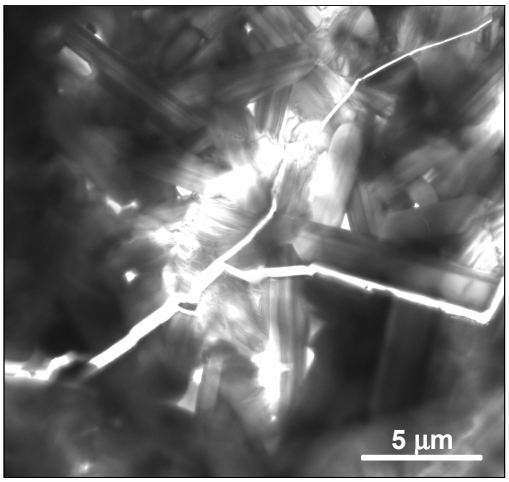

Fig. 9: Cracks in the sample after holding at 1900°C for 5 min.

IV. DISCUSSION

In the above section, we have demonstrated that the amorphous Al-O-Si-C IGFs in ABC-SiC started to crystallize at ~1000°C, and fully crystallized above 1100°C. These results agreed well with the experimental work by Rouxel *et al*, in which partial crystallization was observed in the bulk SiOC glasses at >1150°C, and the crystallization was more completed at 1300°C.[31] The similar amorphous-to-crystalline transitions in the two systems may be attributed to the similar elemental constituents. Indeed, the crystallization temperature (~1000°C) of the amorphous IGFs studied in the present work is lower than that of the bulk SiOC glasses, presumably because of the presence of Al and the close to two-dimensional geometry of the IGFs. Another fact worthy of note is the high stability of the crystallized IGF structure: about 60% crystallized IGFs survived the short-time 1900°C treatment. Considering that one of the IGF structures was determined to be Al_2OC-like with SiC solid solution,[11] the stable IGF structure at high temperature would not be in agreement with the conclusion by Lihrmann *et al.* that Al_2OC structure tended to decompose at >1200°C, following a chemical reaction of $4Al_2OC \rightarrow Al_4O_4C + Al_4C_3$.[32] It is possible that the observed transport of Al-C from nanoprecipitates into the IGFs at temperature above 1200°C impeded the decomposition reaction in ABC-SiC.

Nagano *et al*. reported that SiC sintered with Al additives lost weight at 1800°C in argon atmosphere, and attributed the weight loss to vaporization of the grain boundary

phase, the decomposition of SiC, as well as eroded surface.[26] Our experiments confirmed minor dissolution of SiC grains and somewhat reduction in the amount of grain boundary material (narrower IGFs) at 1900°C in the near-to-surface areas. However, a large number of empty triple-junction pockets are more likely to cause the noticeable weight loss. What remained to be mysterious is that those thermal effects seen in samples after the 1900°C treatment did not present in the as-processed samples which after all were hot-pressed at 1900°C. Much of the effects would therefore be related to the near-to-surface features or have to be associated with evaporative processes that are suppressed in the closed die used in hot pressing.

V. CONCLUSIONS

Systematic TEM characterization has been performed on hot-pressed ABC-SiC samples annealed between 800°C and 1600°C, and at 1900°C. It was found that thermal treatment above 1000°C crystallized the amorphous intergranular films. At about 1300°C, Al diffusion in SiC lattice became significant, resulting in the formation of uniformly dispersed, nanoscale precipitates inside SiC grains. The lattice diffusion led to enrichment of the Al content in the IGFs.

At 1600°C, evidence of volatilization could be found in triple junction pore formation due to evaporation of secondary phase particles. The IGFs survived the 5 min treatment at 1900°C, but at least 25% of the IGFs re-melted, with no significant changes in chemical constituents compared to that in 1500°C-annealed samples. Other structural responses to the 1900°C-heating include dissolution of the nanoprecipitates, evaporation of secondary-phase particles, unit cell dilation, as well as extensive cracking in near free-surface regions. It can be concluded that ABC-SiC is a good candidate material for structural application at up to 1500°C.

ACKNOWLEDGMENT:

This work was supported by the Director, Office of Science, Office of Basic Energy Sciences, Division of Materials Sciences and Engineering of the U.S. Department of Energy under Contract No. DE-AC03-76SF0098. Part of this work was made possible through the use of the National Center for Electron Microscopy facility at the Lawrence Berkeley National Laboratory. Thanks are due to Qing Yang for her help in processing the SiC samples.

REFERENCES

1. T. Mitchell, Jr., L.C. Dejonghe, W.J. MoberlyChan, and R.O. Ritchie, J. Am. Ceram. Soc. **78**, 97 (1995).

2. P.F. Becher, J. Am. Ceram. Soc. **74**, 255 (1991).

3. P.F. Becher, E.Y. Sun, K.P. Plucknett, K.B. Alexander, C.H. Hsueh, H.T. Lin, S.B. Waters, and C.G. Westmoreland, J. Am. Ceram. Soc. **81**, 2821 (1998).

4. J.J. Cao, W.J. MoberlyChan, L.C. De Jonghe, C.J. Gilbert, and R.O. Ritchie, J. Am. Ceram. Soc. **79**, 461 (1996).

5. N. P. Padture, "In Situ-Toughened Silicon Carbide," J. Am. Ceram. Soc. **77**, 519 (1994).

6. F.F. Lange, J. Mater. Sci. **10**, 314 (1975).

7. R. Hamminger, G. Grathwohl, and F. Thummler, J. Mater. Sci. **18**, 353 (1983).

8. L. Sigl, and H.-J. Kleebe, J. Am. Ceram. Soc. **76**, 773 (1993).

9. W.J. MoberlyChan, J.J. Cao, and L.C. De Jonghe, Acta Mater. **46**, 1625 (1998).

10. W.J. MoberlyChan, and L.C. De Jonghe, Acta Mater. **46**, 2471 (1998).

11. X.F. Zhang, M.E. Sixta, and L.C. De Jonghe, J. Am. Ceram. Soc. **83**, 2813 (2000).

12. J.-L. Huang, A.C. Hurford, R.A. Cutler, and A.V. Virkar, J. Mater. Sci. Lett. **21**, 1448 (1986).

13. A.K. Misra, J. Am. Ceram. Soc. **74**, 345 (1991).

14. C.J. Gilbert, J.J. Cao, L.C. De Jonghe, and R.O. Ritchie, J. Am. Ceram. Soc. **80**, 2253 (1997).

15. K.T. Faber, and A.G. Evans, Acta Metall. **31**, 565 (1983).

16. K.T. Faber, and A.G. Evans, Acta Metall. **31**, 577 (1983).

17. P.F. Becher, C.H. Hsueh, P. Angelini, and T.N. Tiegs, J. Am. Ceram. Soc. **71**, 1050 (1988).

18. D. Chen, C.J. Gilbert, X.F. Zhang, and R.O. Ritchie, Acta Mater. **48**, 659 (2000).

19. D. Chen, X.F. Zhang, and R.O. Ritchie, J. Am. Ceram. Soc. **83**, 2079 (2000).

20. D. Chen, M.E. Sixta, X.F. Zhang, L.C. De Jonghe, and R.O. Ritchie, Acta Mater. **48**, 4599 (2000).

21. X.F. Zhang, M.E. Sixta, and L.C. De Jonghe, J. Mater. Sci. **36**, 5447 (2001).

22. R.O. Ritchie, D. Chen, and X.F. Zhang, Int. J. Mater. Prod. Tech. **1**, 331 (2001).

23. X.F. Zhang, M.E. Sixta, and L.C. De Jonghe, Defect and Diffusion Forum **186-187**, 45 (2000).

24. M.E. Sixta, X.F. Zhang, and L.C. De Jonghe, J. Am. Ceram. Soc. **84**, 2022 (2001).

25. X.F. Zhang, G.Y. Lee, D. Chen, R.O. Ritchie, and L.C. De Jonghe, J. Am. Ceram. Soc. in press.

26. T. Nagano, K. Kaneko, G.-D. Zhan, and M. Mitomo, J. Am. Ceram. Soc. **83**, 2781 (2000).

27. X.F. Zhang, Q. Yang, L.C. De Jonghe, and Z. Zhang, J. Microsc. **207**, 58 (2002).

28. H. Ribes, M. Suery, G. L'Esperance, and J.G. Legoux, Metall. Trans. **21A**, 2489 (1990).

29. X.F. Zhang, M.E. Sixta, and L.C. De Jonghe, J. Am. Ceram. Soc. **84**, 813 (2001).

30. I.B. Cutler, P.D. Miller, W. Rafaniello, H.K. Park, D.P. Thompson, and K.H. Jack, Nature **275**, 434 (1978).

31. T. Rouxel, G-.D. Soraru, and J. Vicens, J. Am. Ceram. Soc. **84**, 1052 (2001).

32. J.M. Lihrmann, T. Zambetakis, and M. Daire, J. Am. Ceram. Soc. **72**, 1704 (1989).

Table I: EDS-determined Al concentration in SiC grains (Al/SiC wt%), Al excess in grain boundary films (Γ_{Al}), as well as C/Si atom ratio in samples annealed at 1500°C and the same bulk piece subsequently fired at 1900°C. Statistical mean values are listed with standard deviations.

Samples ABC-SiC	**Al/SiC** (wt%)	Γ_{Al} (nm^{-2})	**C/Si** (atom ratio)
1500°C-168 hrs	1.6±0.2	19.7±9.5	1.23±0.20#
1900°C–5 min.	1.4±0.1	16.4±4.5	0.94±0.36

#Hydrocarbon contamination during EDS spectrum acquisition caused a greater C/Si mean value.

Table II: Lattice parameters determined using selected-area electron diffraction. 4H- and 6H-SiC grains were analyzed. Experimental errors are adopted. Volume dilation for the unit cells after annealing is calculated with respect to the as-hot-pressed samples.

ABC-SiC	**α-4H ($P6_3mc$)**	**α-6H ($P6_3mc$)**
As-Hot-Pressed		
a (Å)	3.07±0.03	3.06±0.03
c (Å)	10.03±0.21	14.89±0.38
1500°C-168 hrs		
a (Å)	3.08±0.03	3.08±0.03
c (Å)	9.99±0.21	15.02±0.24
Volume Dilation	Negligible	Negligible
1900°C-5 min#		
a (Å)	3.19±0.04	3.06±0.03
c (Å)	10.44±0.23	15.66±0.26
Volume Dilation	12.4±9.9 %	5.2±4.5 %

#From the same bulk sample first annealed at 1500°C for 168 hrs and cooled.

Figure captions:

Fig. 1: General microstructural morphology of as-hot-pressed ABC-SiC.

Fig. 2: Three high-resolution images taken from an ABC-SiC sample annealed at 1000°C for 5 hrs. IGFs with (a) amorphous, (b) partially ordered, and (c) crystallized structures can be seen.

Fig. 3: (a), High-resolution image of an amorphous IGF in as-hot-pressed ABC-SiC. (b), The same IGF as in (a) but after in-situ heating in a transmission electron microscope at 1200°C for 25 hrs. Arrows indicate the discrete, crystallized IGF segments. The high-resolution image in (b) was taken at room temperature.

Fig. 4: Nanoprecipitates formed in an ABC-SiC sample annealed at 1400°C. Precipitate-depletion zone along the grain boundary can be seen.

Fig. 5: Plots of EDS-determined Al site density in grain boundary films (N_{Al}^{GB}) and in SiC matrix grains (Al/SiC, wt%) as a function of annealing temperature. Standard deviations are given.

Fig. 6: A secondary-phase particle in the 1400°C-annealed sample. Note the second phase separation within the particle.

Fig. 7: Empty triple-pockets observed in ABC-SiC samples after the thermal treatment at 1600°C. Note the 100% occupied triple-pockets in as-hot-pressed samples, Fig. 1.

Fig. 8: High-resolution micrographs obtained from (a), the as-hot-pressed sample, (b), the 1500°C-annealed sample, (c) and (d), the 1900°C-treated sample. The 1500°C treatment crystallized the amorphous IGF, while the subsequent brief holding at 1900°C re-melted some crystalline IGFs. Note that the images were not taken from the same IGF.

Fig. 9: Cracks in the sample after holding at 1900°C for 5 min.